CZECH TECHNICAL UNIVERSITY IN PRAGUE

FACULTY OF MECHANICAL ENGINEERING
DEPARTMENT OF PROCESS ENGINEERING

MODEL of the PLATE HEAT EXCHANGER
DIPLOMA THESIS

2015 MEHMET AYAS

Annotation sheet

Name: Mehmet

Surname: Ayas

Title Czech:

Title English: Model of Plate Heat Exchanger

Scope of work: number of pages: 65

Number of figures: 33

Number of tables: 21

Number of appendices: 3

Academic year: 2014-2015

Language: English

Department: Process Engineering

Specialization: Process Engineering

Supervisor: Ing. Jan Skocilas Ph.D

Reviewer:

Tutor:

Submitter: Czech Technical University in Prague, Faculty of Mechanical Engineering,

Department of Process Engineering

Annotation - Czech:

Annotation - English: Design a model of plate heat exchanger in software ANSYS. Perform a simulation for given operational parameters. Compare the results of the simulation with experimental data. Experimental data will be obtained from measurement on the real model of heat exchanger connected to pipeline system.

Keywords: Simulation, Heat exchanger, Heat transfer

Utilization:

CONTENTS

Declaration

I confirm that the diploma (Master's) work was disposed by myself and independently, under leading of my thesis supervisor. I stated all sources of the documents and literature.

In Prague…….. ……..

Name and Surname

Acknowledgments

I dedicate this study to my family for their patience and to endure me.

I would like to thank Ing. Jan Skocilas Ph.D for his advice, interest and great support.

ABSTRACT

This study is focused on the designing of chevron type plate heat exchanger in the ANSYS software. Geometry has been constructed in Solidworks software with respect to catalogue values. Then 2 different mesh models have been created with different quality and different number of elements. These two models have been simulated and results were compared with experimental data. Results were nearly satisfied for pressure drop values but results for outlet temperatures and heat fluxes were different.

Keywords: ANSYS simulation, Pressure Drop, Analytical and Numerical Solutions.

NOMECLATURE

A_s	Heat transfer area [m^2]
b	Channel spacing [mm]
C	Heat capacity [W/K]
c_p	Specific heat [J/(kg-K)]
D_e	Equivalent diameter [mm]
D_h	Hydraulic diameter [mm]
D_p	Port diameter [mm]
f	Friction factor [-]
h	Heat transfer coefficient [W/(Km^2)]
k	Thermal conductivity [W/(mK)]
L	Plate length [mm]
G	Mass velocity [kg/(m^2s)]
m	Mass flow rate [kg/s]
N	Number of plates [-]
N_p	Number of passes [-]
Nu	Nusselt number [-]
NTU	Number of units [-]
P	Pressure [Pa]
ΔP	Pressure drop [Pa]
Pr	Prandtl number [-]
R	Thermal resistance [W/K]
Re	Reynolds number [-]
Q	Heat transfer rate [W]
t	Plate thickness [mm]
T	Temperature [K]

ΔT_{lm}	Log mean temperature difference [K]
U	Overall heat transfer coefficient [W/(Km^2)]
w_p	Width between ports [mm]
$\dot{V}$	Volume flow rate (m^3/s)

α	Thermal diffusivity [m^2/s]
β	Corrugation inclination angle [^{o}]
ϕ	Surface enlargement factor
ρ	Density [kg/m^3]
μ	Dynamic viscosity [Pa.s]
ν	Kinematic viscosity [m^2/s]

1. INTRODUCTION

Heat exchanger is a device that is used for transfer thermal energy from one liquid to another that are at different temperatures, while usually preventing them mixing each other. Heat exchangers are used in a wide variety of applications such as HVAC systems, food and chemical process systems, heat recovery systems.

This work is based on comparing of real gasketed plate heat exchanger with numerical model. Firstly we will find required dimensions for designing plate model according to given parameters by using analytical methods and then determined model will be simulated by using ANSYS Fluent software.

2. KNOWLEDGE about PLATE HEAT EXCHANGER

Plate heat exchanger consists of a series of parallel rectangular plates which are corrugated to increase turbulence and to give mechanical rigidity. Also increasing turbulence provides greater value of heat transfer coefficient. The hot and cold fluids flow in alternate passages, and thus each cold fluid is surrounded by two hot fluid streams or vice versa. That arrangement induces very effective heat transfer. Capacity of this type of heat exchangers can be changed by adding or removing number of plates. Generally, these exchangers cannot accommodate very high pressures, temperatures, or pressure and temperature differences. Plate heat exchangers can be classified as gasketed, brazed or welded (which are most commonly used plate heat exchangers), spiral, lamella and plate coil.

2.1. Gasketed Plate Heat Exchangers

The most commonly used plate heat exchanger type in which parallel plates with gaskets between plates provide fluid seal is shown in Figure 1[6]. Gasketed plate heat exchanger consists of a number of thin rectangular metal plates sealed around the edges by gaskets and held together in a frame.

The frame usually has a fixed end cover (headpiece) fitted with connecting ports and a movable end cover (pressure plate, follower, or tailpiece). In the frame, the plates are suspended from an upper carrying bar and guided by a bottom carrying bar to ensure proper alignment. For this purpose, each plate is notched at the centre of its top and bottom edges. The plate pack with fixed and movable end covers is clamped together by long bolts, thus compressing the gaskets and forming a seal.

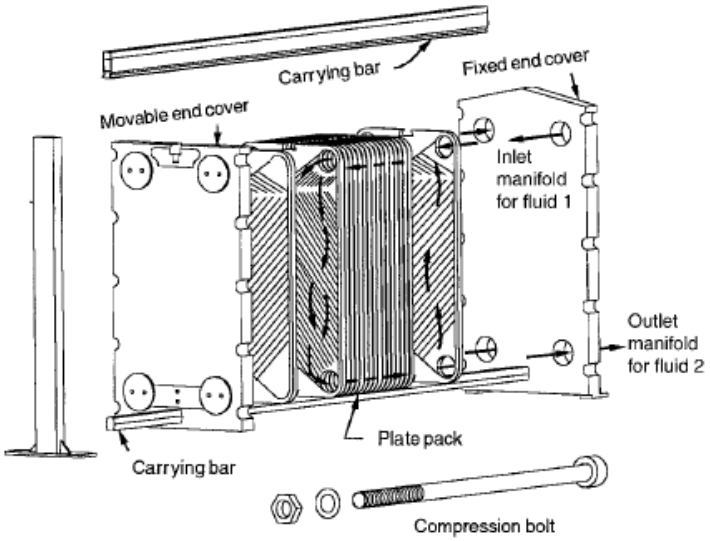

Figure 1. (Gasketed plate heat exchanger)

Each plate is made by stamping a corrugated (or wavy) surface pattern on sheet metal. On one side of each plate, special grooves are provided along the periphery of the plate and around the ports for a gasket shown in Figure 2 [6].

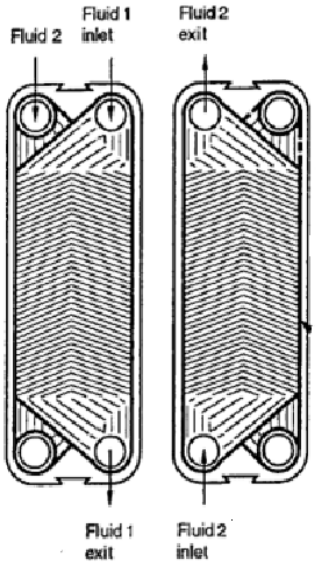

Figure 2. (Plates of plate heat exchanger)

The corrugations on successive plates contact or cross each other to give mechanical support to the plate pack through a large number of contact points. The resulting flow passages are narrow, highly interrupted, and tortuous, and enhance the heat transfer rate and decrease fouling

resistance by increasing the shear stress, producing secondary flow, and increasing the level of turbulence. The corrugations also improve the rigidity of the plates and form the desired plate spacing.

This can take apart and access all working surfaces for inspection and cleaning .Its applications are limited to be between -30 and 200 ^{o}C with pressure drop up to 20 bar.

2.2. Welded (Brazed) Plate Heat Exchangers

The limitations of the gasketed plate heat exchangers can be overcome by welding the plates together. That eliminates both gaskets and frame from the design. Elimination of the gaskets improves application ranges of temperature and pressure. The operating temperature range varies between -200 and 900 ^{o}C and for pressure up to 3 MPa. An important limitation is that they can only be cleaned chemically and not mechanically.

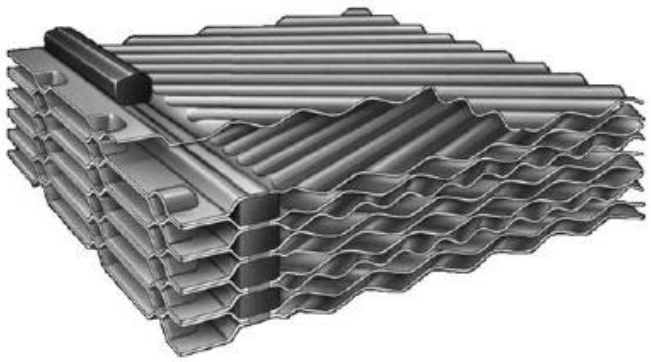

Figure 3 (Cross section of welded plate heat exchanger).[7]

2.3. Advantages and Limitations

Some advantages of plate heat exchangers are as follows.

- They can easily be taken apart into their individual components for cleaning, inspection and maintenance.
- The heat transfer surface area can easily be changed or rearranged for a different task.
- High shear rates and shear stresses, secondary flow, high turbulence, and mixing due to plate corrugation patterns reduce fouling to about 10 to 25% of that of a shell-and-tube heat exchanger, and enhance heat transfer.

- The gross weight of a plate exchanger is about one sixth that of an equivalent shell-and-tube heat exchanger.
- The residence time for different fluid particles or flow paths on a given side is approximately the same. That is desirable for uniformity of heat treatment in applications such as sterilizing, pasteurizing.

Some disadvantages of plate heat exchangers are given below.

- The plate exchanger is capable of handling up to a maximum pressure of about 3 MPa gauge but is usually operated below 1.0 MPa
- The gasket materials restrict the use of PHEs in highly corrosive applications. They also limit the maximum operating temperature to 260 ^{o}C but are usually operated below 150^{o}C to avoid the use of expensive gasket materials.
- Gasket life is sometimes limited. Frequent gasket replacement may be needed in some applications.
- For equivalent flow velocities, pressure drop in a plate exchanger is very high compared to that of a shell-and tube exchanger.
- Plate heat exchangers are not suitable for erosive duties or for fluids containing fibrous materials.

2.4. Flow Arrangement

The fluid temperatures in heat exchangers generally vary along their flow path, even the case of constant thermal resistance because of flow distribution and temperature gradient variations across the plates. For that reason, flow configurations have major effect on heat exchanger parameters (temperature, pressure drop, etc)

Parallel flow arrangement; hot and cold fluid streams flowing in same direction; *counter flow arrangement* with fluids flowing opposite directions shown in figure 4*; multi-pass flow arrangement* where fluid streams pass through once in parallel and once in counter flow.

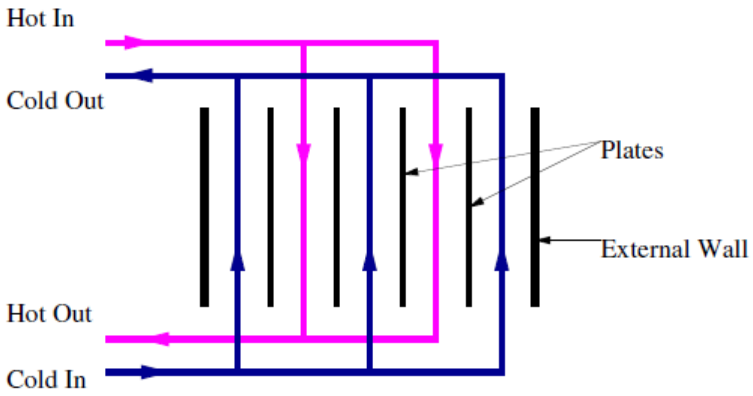

Figure 4 (Counter flow arrangement)

There are also two different types of single pass arrangement which are U and Z arrangement types which is shown in Figure 6 and 7 [8].

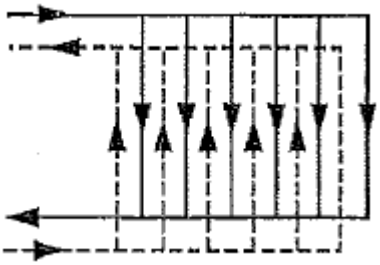

Figure 5 (U arrangement)

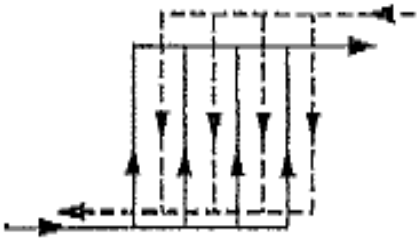

Figure 6 (Z arrangement)

2.5.Plate Heat Exchanger Corrugation

A wide range of types of corrugation is used in plate design. The function of corrugation is to induce turbulence and increasing the heat transfer area. High turbulence results in a very high transfer coefficient, especially compared to shell and tube heat exchangers for similar duties.

There are more than 60 different plate patterns have been developed worldwide. The most widely used corrugations are intermating and chevron corrugation types.

2.5.1. Intermating Type Plate (Washboard Design)

The corrugations are pressed to a depth greater than compressed gasket depth. When the machine is closed, the corrugations fit into on another.

The cross-section of two neighbouring plates, perpendicular the flow direction. Dimples provide interpolate contact and maintain the channel gaps.

The flow gap "*b*" varies from 3 mm to 5 mm with the minimum flow gap c between 1.5 mm and 3 mm, which is shown in figure 7 [7] below.

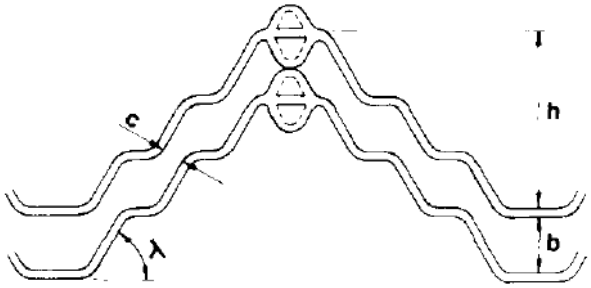

Figure 7 (Intermating type plate)

2.5.2. Chevron Corrugation

Chevron type is the most common corrugation in use today. The corrugations are pressed to same depth as the plate spacing. The chevron angle is reversed on adjacent plates that when the plates are clamped together and the corrugations cross another to provide numerous contact points. Therefore chevron type has greater strength then intermating type which enables it to withstand higher pressure with smaller plate thickness. The corrugation depths on typical plates vary from about 3 to 5 mm.

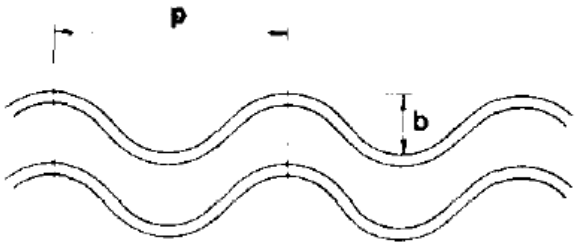

Figure 8(Chevron corrugation) [7].

The thermal-hydraulic performance is strongly influenced by its surface geometry, which is characterized by;

- Corrugation plate
- Corrugation inclination angle between adjacent plates
- Corrugation pitch (p)
- Corrugation height (H)
- Surface enlargement factor

Each plate has four corner ports that provide access to the flow passages on either side of the plate. Corrugation inclination angle (chevron angle) β can be between 0^o and 90^o, typically with 30°, 45 °, or 60 °.

2.6. Geometry

The corrugations increase the surface area of the plate compared to original flat area. To express the increase of developed length to projected length, surface enlargement factor $\emptyset$;

$$\emptyset = \frac{\text{developed length}}{\text{projected length}}$$

$\emptyset$ is the function of corrugation pitch and corrugation depth (plate pitch).

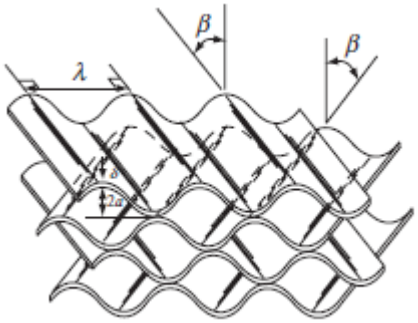

Figure 9 (Plate corrugation) [6].

In the figure above, λ is size of corrugation pitch, 2a (b) is mean channel spacing and all units are *mm.*

The mean channel spacing *b*, between two plates

$$b = p - t \qquad (1)$$

Where *p* is plate pitch or the outside depth of corrugated plate and *t* is the thickness of the plate. Channel spacing *b*, is necessary for calculation of mass velocity and Reynolds number.

The plate pitch is determined from the compressed plate patch length (between the head plates*)* L_c and total number of plates.

$$p = \frac{L_c}{N_t} \qquad (2)$$

In order to calculate corrugation pitch, we can use following equation

$$\emptyset \cong \frac{1}{6}\left(1+\sqrt{1+x^2}+4\sqrt{1+\frac{x^2}{2}}\right) \qquad (3)$$

Where x is:

$$x = \frac{b\,\pi}{\lambda} \qquad (4)$$

Hydraulic Diameter (mm): The hydraulic diameter of channel D_h:

$$D_h = \frac{2b}{\emptyset} \qquad (5)$$

Equivalent Diameter (mm):

$$D_e = 2b \qquad (6)$$

2.7. Development of Analytical Correlations

2.7.1. Mass Velocities

The channel mass velocity is:

$$G = \frac{\dot{m}}{bW_p} \qquad (7)$$

Where W_p is width of the plane.

Mass velocity is at ports:

$$G_p = \frac{4\dot{m}}{\pi {D_p}^2} \qquad (8)$$

Where D_p is the diameter of the ports (mm)

2.7.2. Thermal Equations

2.7.2.1. Thermal Diffusivity

Thermal property of the material represents how fast heat diffuses through a material (m^2/s), denoted by α.

$$\alpha = \frac{k}{\rho * c} \qquad (9)$$

In the equation, k is thermal conductivity (W/[K*m]), ρ is density (kg/m^3) and c is specific heat (kJ/[kg*K])

2.7.2.2. Prandtl Number

The relative thickness of the velocity and thermal boundary layers are described by Prandtl number (*Pr*):

$$Pr = \frac{Molecular\ diffusivity\ of\ momentum}{Molecular\ diffusivity\ of\ heat}$$

$$Pr = \frac{\vartheta}{\alpha} = \frac{\mu * c}{k} \qquad (10)$$

In the equation μ is dynamic viscosity *(Pa*s)* and ϑ is kinematic viscosity *(m^2/s)*

- Heat diffuses quickly , if *Pr*<1 and slowly if *Pr* >1
- If we want to keep temperature at desired range during transportation through pipe, high *Pr* number liquids are preferred such as oil

2.7.2.3. Reynolds Number (Re)

Ratio of the inertia force to viscous forces in the fluid which is used for specifying the fluid has laminar or turbulent characteristic. The transition from laminar flow to turbulent flow (Reynolds number) depends on surface geometry, roughness, flow velocity surface temperature and type of the fluid. For plate heat exchangers, Reynolds number for turbulent flow is over the 1000 and below this value exhibits laminar flow characteristics.

$$Re = \frac{Inertia\ forces}{Viscous\ forces}$$

$$Re = \frac{V * L_c}{\vartheta} = \frac{\rho * V * L_c}{\mu} \qquad (11)$$

Where ρ is density (m^3/s), V is mean velocity of stream (m/s) and L_c is characteristic length (mm).

Reynolds number in terms of mass velocity is:

$$Re = \frac{GD_h}{\mu} \qquad (12)$$

In equation G is mass velocity ($kg/[m^2*s]$).

2.7.2.4. Area Density (β)

The ratio of heat transfer surface of heat exchanger to its volume is known *as area density*. (m^2/m^3)

A heat exchanger with β>700 (m^2/m^3) is classified as being compact.

2.7.2.5. Nuselt Number (Nu)

In convection studies, it is common practice to non-dimensionalize the governing equations and combine the variables, which group together into dimensionless numbers in order to reduce the number of total variables. It is also common practice to non-dimensionalize the heat transfer coefficient *h* with the Nusselt number, defined as

$$Nu = \frac{hL_c}{k} \qquad (13)$$

Where k is thermal conductivity of fluid and L_c is characteristic length.

2.7.2.6. Heat Capacity Rate (*C*)

Product of mass flow rate and the specific heat of a fluid; ($W/^oC$)

$$C = \dot{m}c_p \qquad (14)$$

A heat exchanger typically involves two flowing fluids separated by a solid wall. Heat is transferred from the hot fluid to the wall by convection, thorough the wall by conduction and from the wall to cold fluid again by convection.

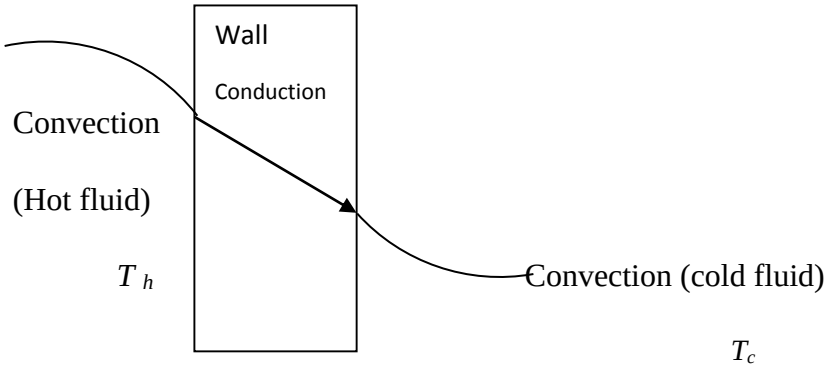

Figure 10 (Heat transfer mechanism)

Assumptions about thermal calculation:

- Heat exchangers usually operate for long periods of time with no change in their operation conditions. Therefore they can be modelled as steady –flow devices.
- Change in velocities and elevations of the fluid streams are so small thus, potential and kinetic energy changes are negligible.
- Outer surface of heat exchanger is considered as perfectly insulated.

2.7.2.7. Overall Heat Transfer Coefficient

A heat exchanger typically involves two flowing fluids separated by a solid wall. Heat is first transferred from the hot fluid to the wall by convection, through the wall by conduction, and from the wall to cold fluid again by convection.

In heat exchanger analysis, it is very convenient to combine all thermal resistance in the path of heat flow from hot fluid to cold fluid into a single resistance *R*

$$\dot{Q} = \frac{\Delta T}{R} = A_s U \Delta T \qquad (15)$$

Where *R* is thermal resistance ($^oC/W$), ΔT is temperature difference (^oC) and $\dot{Q}$ is heat transfer rate (*W*). In the right side of equation, A_s is the surface area and *U* is the overall heat transfer coefficient which unit is W/($m^{2.}$K)

Equivalent resistance is sum of the resistances due to conduction and convention.

$$R_{tot} = R_{c,h} + R_{cond} + R_{c,c} \qquad (16)$$

Where $R_{c,h}$ and $R_{c,c}$ thermal resistances due to convection in cold and hot sides. R_{cond} is thermal resistance due to convection. If we substitute equation and 6 and 7 and cancelling ΔT in equation 6, we obtain following equations.

$$\frac{1}{U * A_s} = R_{tot} \qquad (17)$$

$$\frac{1}{R_{tot} * \mathrm{A}} = \frac{1}{h_c * A_c} + \frac{1}{h_h * A_h} + \frac{\delta}{k * A} \qquad (18)$$

For plate heat exchanger heat transfer surfaces are almost identical (A_h=A_c). After canceling of areas in the equations above, we obtain following equation 19.

$$\frac{1}{U} = \frac{1}{h_c} + \frac{1}{h_h} + \frac{\delta}{k} \qquad (19)$$

Where *U* is overall heat transfer coefficient and unit is *W/(m^{2}K).*

According to first law of thermodynamic over the control volume of any two fluids, rate of heat transfer of hot and cold streams equal each other.

$$Q=mc\Delta T \quad (20)$$

$$Q=m_c*c_c*\Delta T_c= =m_h*c_h*\Delta T_h \qquad (21)$$

Here m_c and m_h are flow rates of hot and cold fluid streams, c_c and c_h are heat capacities and ΔT is temperature difference.

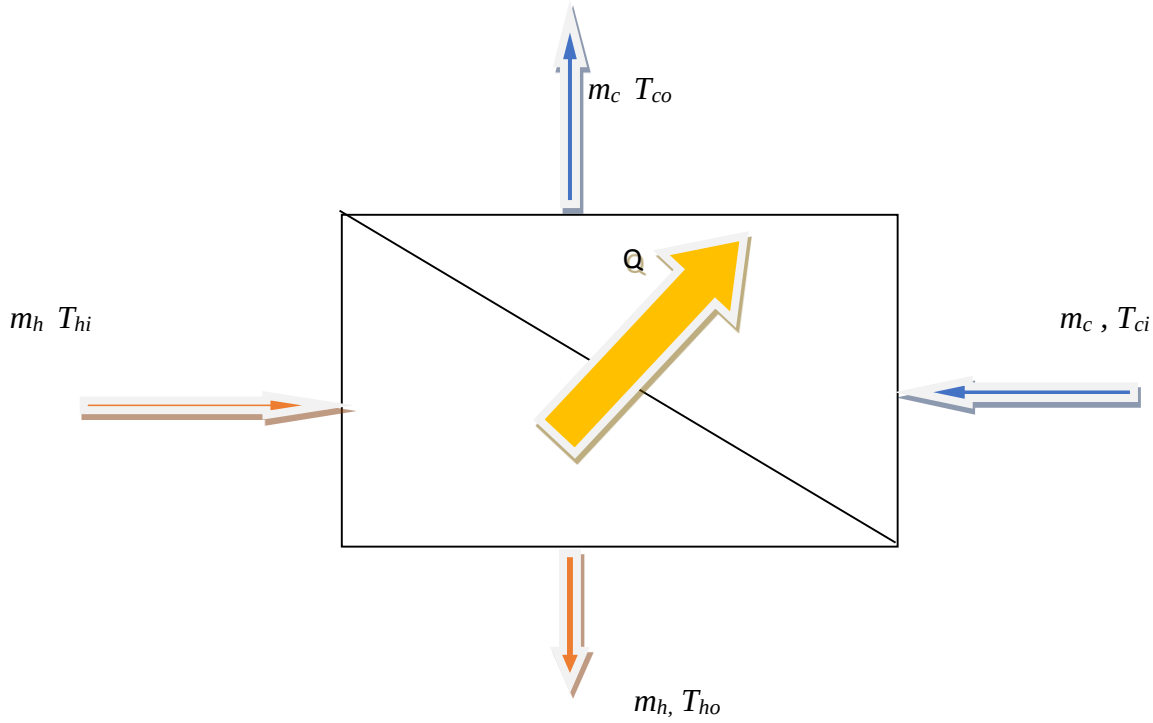

Figure 11 (Heat transfer through plate)

Direction of the Q is from hot fluid to cold one according to second law of thermodynamic. In addition, two special types of heat exchangers are condenser and boiler and in which one fluid undergoes phase change, for that reason, the temperature of the one fluid stream in heat exchanger remains constant. In two cases, pressure is constant due to phase change process.

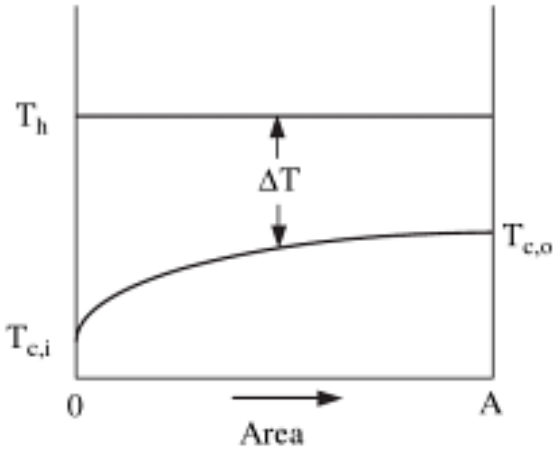

Figure 12 (Temperature distribution of condenser) [9].

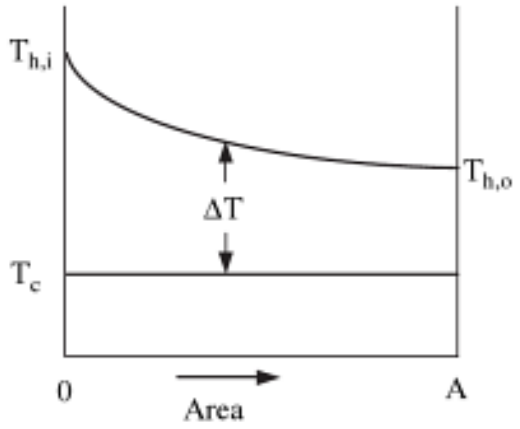

Figure 13 (Temperature distribution of evaporator)[9].

2.7.2.9. Fouling Factor

Accumulation of deposits on the surface creates additional resistance on heat transfer surface and effect of that accumulation is expressed by fouling factor which is measure of thermal resistance introduced by fouling and that decreases heat exchanger performance adversely.

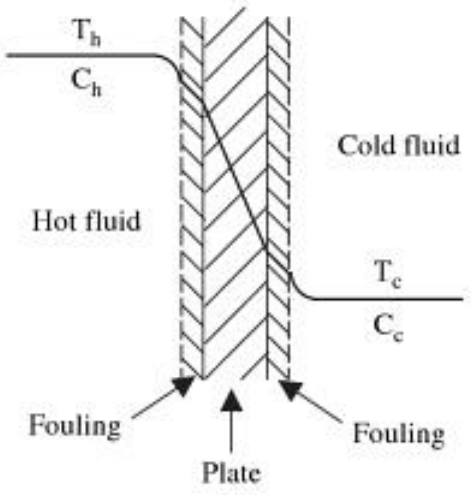

Figure 14 (Fouling resistance) [9].

$$\frac{1}{U} = \frac{1}{h_h} + \frac{1}{h_c} + \frac{\delta}{k} + R_{f,g} + R_{f,c} \qquad (22)$$

In the formula, $R_{f,h}$ and $R_{f,c}$ represent heat transfer resistances for hot and cold fluid sides due to fouling.

2.7.2.10. Log Mean Temperature Difference (LMTD)

There are some methods for thermal design of heat exchanger and one of them is LMTD method. This method is quite suitable for determining the size of heat exchanger when mass flow rates, inlet and outlet temperatures of hot and cold streams are specified.

The rate of heat transfer from hot fluid stream to cold fluid stream is expressed as:

$$\dot{Q} = U * A_s * \Delta T_{lm} \quad (23)$$

Here A_s is heat transfer surface and ΔT_{lm} is log mean temperature difference. Along the heat transfer surface, temperature difference is not constant between hot and cold fluids, it varies through the path of fluid stream,

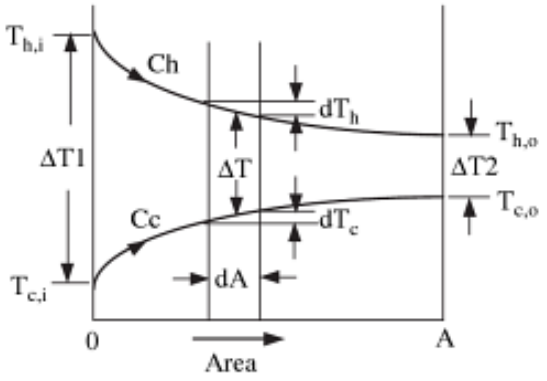

Figure 15 (Temperature variation along parallel flow) [7].

$$\Delta T_{lm} = \frac{(\Delta T_1 - \Delta T_2)}{\ln(\frac{\Delta T_1}{\Delta T_2})} \quad (24)$$

Where ΔT_1 and ΔT_2 are temperature differences between ends of heat exchanger.

$\Delta T_1 = T_{hi} - T_{ci}$

$\Delta T_2 = T_{ho} - T_{co}$ for parallel flow

$\Delta T_1 = T_{hi} - T_{co}$

$\Delta T_2 = T_{ho} - T_{ci}$ for counter flow

It is important that, ΔT_{lm} is always less than ΔT_{am} (average mean temperature)

$$\Delta T_{am} = \frac{\Delta T_1 + \Delta T_2}{2} \qquad (25)$$

$\Delta T_{lm} < \Delta T_{am}$ (always)

Note that, if we compare a parallel flow and counter flow arrangement with same heat transfer surface area, and specified inlet and output temperatures, log mean temperature difference for counter flow heat exchanger is always greater than parallel flow heat exchanger.

$\Delta T_{lm,\,cf} > \Delta T_{lm,\,pf}$

In order to achieve the same heat transfer rate, smaller surface is needed for same value of overall heat transfer coefficient. That makes counter flow heat exchanger more efficient than parallel flow heat exchanger for same parameters.

Other essential aspect of the parallel flow arrangement is that the final temperature of cold fluid stream is always less than outlet hot fluid stream temperature.

In counter flow arrangement, on the other hand, the final cold fluid temperature may exceed the outlet temperature of hot fluid stream.

2.7.3. Heat Transfer and Pressure Drop Calculations

In this section, enhanced thermal-hydraulic characteristics of chevron plates are given.

The heat transfer enhancement strongly depends on chevron inclination angle β, relative to flow direction. Heat transfer coefficient and friction factor increase with β. On the other hand the performance of a chevron plate also depends on the surface enlargement factor, corrugation profile and gap *b*.

There are numerous correlation to calculate pressure drop and Nusselt number which depend on corrugation geometry, sizes of plate and flow regime.

2.7.3.1. Pressure Drop Calculation

The overall pressure drop of plate heat exchanger consists of the pressure drop at inlet and outlet ports and pressure drop in channels due to friction. The pressure drop due to potential energy lost is neglected in our calculation. The total pressure drop is;

$$\Delta P = \Delta P_{ch} + \Delta P_p \qquad (36)$$

Pressure drop at ports:

$$\Delta P_p = \frac{1.5 N_p {G_p}^2}{2\rho} \qquad (37)$$

G_p: Mass velocity at ports ($\frac{kg}{m^2 s}$)

N_p: Number of passes

The pressure drop at channel due to friction is:

$$\Delta P_{ch} = \frac{2 f L G^2 N_p}{D_h \rho} \qquad (38)$$

Where f is friction factor, L is characteristic length.

There are numerous correlation to determine friction factor *f* and Nusselt number. These correlations are given below.

According to Mulley Correlation [5].

Equation is valid for $Re > 10^3$, $30 \leq \beta \leq 60$ and $1 \leq \emptyset \leq 1.5$

$$f = [2.917 - 0.1277\beta + 2.016 \times 10^{-3}\beta^2] \times [5.474 - 19.02\emptyset + 18.93\emptyset^2 - 5.341\emptyset^3] \times Re^{-[0.2+0.0577 \sin\left[\left(\frac{\pi\beta}{45}\right)+2.1\right]]} \qquad (39)$$

$$Nu = [2.668 - 0.006967\beta + 7.244 \times 10^{-5}\beta^2] \times [20.78 - 50.94\emptyset + 41.16\emptyset^2 - 10.51\emptyset^3] \times Re^{[0.728+0.0543 \sin\left[\left(\frac{\pi\beta}{45}\right)+3.7\right]]} Pr^{\frac{1}{3}} \left(\frac{\mu}{\mu_w}\right)^{0.14} \qquad (40)$$

According to Martin Correlation [8].

The Fanning‘s friction factor *f* is:

$$\frac{1}{\sqrt{f}} = \frac{cos\beta}{\sqrt{0.045tan\beta + 0.09sin\beta + f_o/cos\beta}} + \frac{1 - cos\beta}{\sqrt{3.8f_1}} \qquad (41)$$

Where

$$f_0 = \begin{cases} \frac{16}{Re} & \text{for } Re < 2{,}000 \\ (1.56 \ln Re - 3.0)^{-2} & \text{for } Re > 2{,}000 \end{cases}$$

$$f_1 = \begin{cases} \frac{149.25}{Re} + 0.9625 & \text{for } Re < 2{,}000 \\ \frac{9.75}{Re^{0.289}} & \text{for } Re > 2{,}000 \end{cases}$$

Nusselt Number

$$Nu = 0.205Pr^{\frac{1}{3}}\left(\frac{\mu}{\mu_w}\right)^{\frac{1}{6}}(fRe^2 sin2\beta)^{0.374} \qquad (42)$$

From Table [8].

The Fanning‘s factor *f*

$$f = \frac{K_p}{Re^m} \qquad (43)$$

Nusselt Number:

$$Nu = C_h Re^n Pr^{1/3} \qquad (44)$$

K_p, *m*, C_h *and n* values are given in table below, and note that in the table angel value is (90^o-β)

Constants for Single-Phase Heat Transfer and Pressure Loss Calculation in Gasketed-Plate Heat Exchangers[2,10]

Chevron Angle (degree)	Heat Transfer			Pressure Loss		
	Reynolds Number	C_h	n	Reynolds Number	K_p	m
≤ 30	≤ 10	0.718	0.349	< 10	50.000	1.000
	> 10	0.348	0.663	10–100	19.400	0.589
				> 100	2.990	0.183
45	< 10	0.718	0.349	< 15	47.000	1.000
	10–100	0.400	0.598	15–300	18.290	0.652
	> 100	0.300	0.663	> 300	1.441	0.206
50	< 20	0.630	0.333	< 20	34.000	1.000
	20–300	0.291	0.591	20–300	11.250	0.631
	> 300	0.130	0.732	> 300	0.772	0.161
60	< 20	0.562	0.326	< 40	24.000	1.000
	20–400	0.306	0.529	40–400	3.240	0.457
	> 400	0.108	0.703	> 40	0.760	0.215
≥ 65	< 20	0.562	0.326	50	24.000	1.000
	20–500	0.331	0.503	50–500	2.800	0.451
	> 500	0.087	0.718	> 500	0.639	0.213

Table 1 (Coefficients for pressure drop and Nu number calculation) [8].

3. Computational Fluid Dynamics

Computational fluid dynamics (CFD) is an engineering method for simulating the behaviour of systems, processes and equipment involving flow of gases and liquids, heat and mass transfer, chemical reactions and related physical phenomena. More specifically CFD, or fluid simulation, can be used to reduce pressure drops, to predict aerodynamic lift or drag, to predict the rotor thrust, to calculate the airflow in air conditioned rooms, to ensure adequate cooling, to optimize mixing rates, and so on.

The strategy of CFD is to replace the continuous problem domain with a discrete domain using a grid (Mesh). In the continuous domain, each flow variable is defined at every point in the domain. In the discrete domain, each flow variable is defined only at the grid points.

3.1. ANSYS Fluent

ANSYS Fluent software contains the broad modelling capabilities needed to model flow, turbulence, heat transfer, and reactions for industrial applications ranging from air flow over an artificial wing to combustion in a furnance. Special models that give the software the ability to model in-cylinder combustion, aeroacoustics, turbomachinery, and multiphase systems have served to broaden its reach.

ANSYS CFD solvers are based on the finite volume method. Domain is discretised into a finite set of control volumes and general conservation (transport) equations for mass, momentum, energy, species, etc. are solved on this set of control volumes. Partial differential equations are discretised into a system of algebraic equations and these equations are then solved numerically to render the solution field.

3.1.3. Steps for ANSYS CFD Solutions [12].

1-Identifying of modelling goal: Determination of target of the task, for instance pressure drop or mass flow rate determination.

2-Identification of the domain of the model.

3-Creation of solid model of domain: First step of obtaining a model of fluid domain region which could be two or three dimensional which depends on requirements.

4-Design and creating mesh

A mesh divides a geometry into many elements. These are used by the CFD solver to construct control volumes. Types of used mesh types are given below in figure…

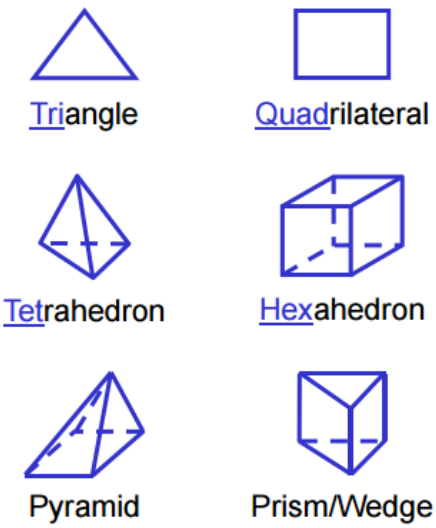

Figure 16 (Mesh Types) [12].

The mesh must resolve geometric features of interest and capture gradients of concern, e.g. velocity, pressure, temperature gradients. For simple geometries, quadrilateral-hexahedron meshes are recommended which can provide higher quality solutions with fewer cells (nodes) than a comparable triangle-tetrahedron mesh types

5-Setting up the solver

For a given problem, following steps must be followed.

- Defining material properties (Fluid, solid or mixture)

- Selection of appropriate physical model (Turbulence, combustion, multiphase, etc.)

- Prescribing operating conditions.

- Prescribing boundary conditions at all boundary zones.

- Providing initial values or a previous solution.

- Setting up solver controls.

- Setting up convergence monitors

6-Computiong Solutions

The discretised conservation equations are solved iteratively until convergence. Convergence is reached when

- Changes in solution variables from one iteration to the next are negligible.
- Overall property conservation is achieved.
- Quantities of interest (e.g. drag, pressure drop) have reached steady values reached steady values.

7-Examining the Results

3.2. LITERATURE SURVEY

This article [2] is about numerical study for hydro-dynamic characteristics and distribution of flow in two cross-corrugated channels of plate heat exchanger. Goal of the study is comparison of the numerical results with the measurements which have been taken by laboratory experiments. The local characteristics around contact points have been discussed and velocity, pressure and flow distribution of the fluid among two channels also have been presented.

Three dimensional simulation of the fluid flow among channels were performed by FLUENT 6.3. The main part of the computational domain is cross corrugated section which is the symmetric with respect to center plane. In order to avoid singularities in the mapping, the line contacts between the upper and lower chevron plates have to be replaced by a surface contact. The grid used for simulation is an unstructured mesh. Tetrahedral elements are created for computational grid to describe the complexity of the cross-corrugated passage. The flow is assumed to be steady, turbulent and three-dimensional. Due to the complex geometry, the turbulent model chosen for simulating the channel is the realizable k-ε model instead of the

standard turbulent k-ε model. Instead of the standard linear-logarithm wall function, the non-equilibrium wall function is used to calculate the variables at the near-wall cells and the corresponding quantities on the wall.

A number of experiments have been conducted for the range of channel Reynolds number from 170 to 1700. It is observed that transition Reynolds number is 430, which is show in figure17.

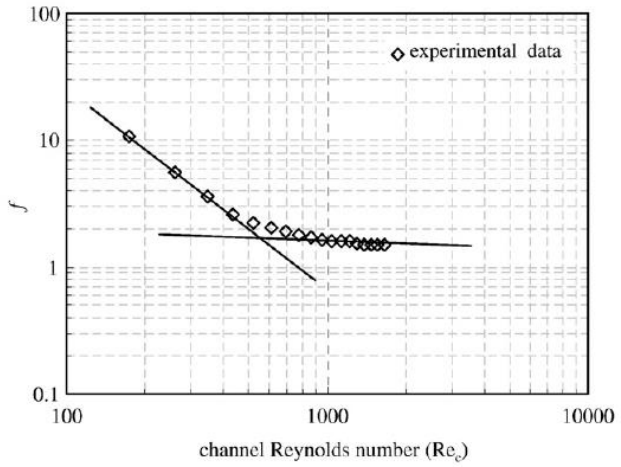

Figure 17 (Reynolds number versus friction factor) [2].

Figure 18 shows the comparison of experimental pressure drops with CFD data for Reynolds number. The deviation of the numerical predictions from experimental data is about 20%. Many secondary flow model is introduced into channels because of complex geometry. This is not well predicted by the realizable k-ε model with the enhanced wall treatment. To improve the accuracy of numerical results, different turbulent models (standard and RNG k-ε models, k-ω standard and SST models) with different boundary treatments have been tried and tested. However, the computational results show that the deviation of the numerical predictions do not get smaller in these cases. The distribution of the fluid from the inlet port into two channels is not uniform by the CFD simulation. The flow rate of the first channel is higher than that of the second channel about 1% in the range of study.

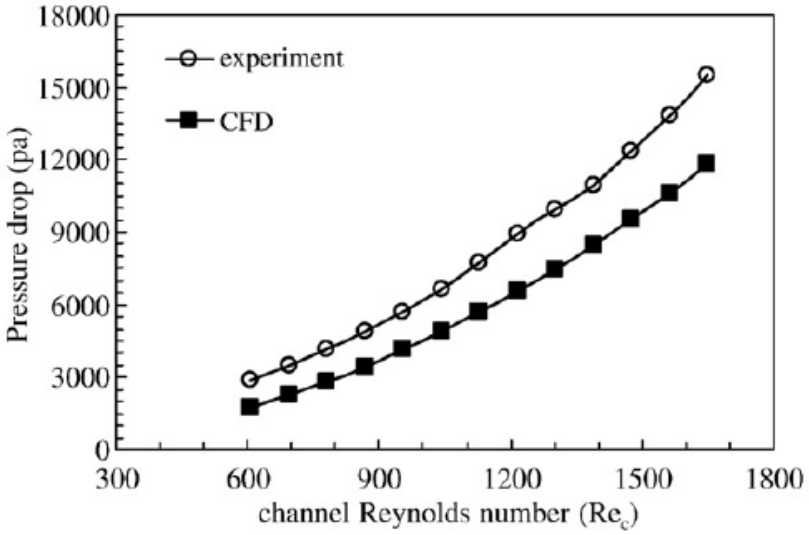

Figure 18 (Reynolds number versus pressure drop) [2].

The article [10] deals with experimental studies of sinusoidal corrugated plate heat exchanger with water as test fluid. Three different plate heat exchanger was used with same geometry and with different corrugation angle as 30^o, 40^o, and 50^o.

It has been observed from the experimental results that the corrugation angle is mainly affecting the pressure drop and the friction factor. As the corrugation angle is increases, the pressure drop of the fluid is found to increase, which results in increase friction factor. Based on this experimental study it can be said that corrugation angle has a major effect on both pressure drop and friction factor. As the corrugation angle increases, pressure drop offered by the channel increases and the friction factor decreases. The increase in pressure drop can be attributed to increase in turbulence occurring in the channel. As the corrugation angle increases, the channel becomes sharper and induces turbulence even at a low flow rate. Results of experiment is given in the figure 19 and 20 below.

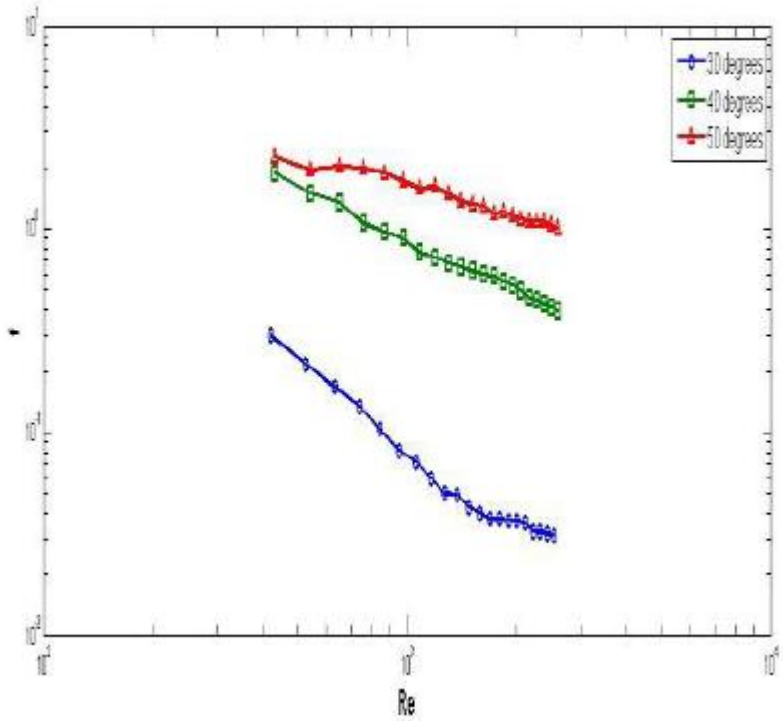

Figure 19 (Reynold number vs friction factor) [10].

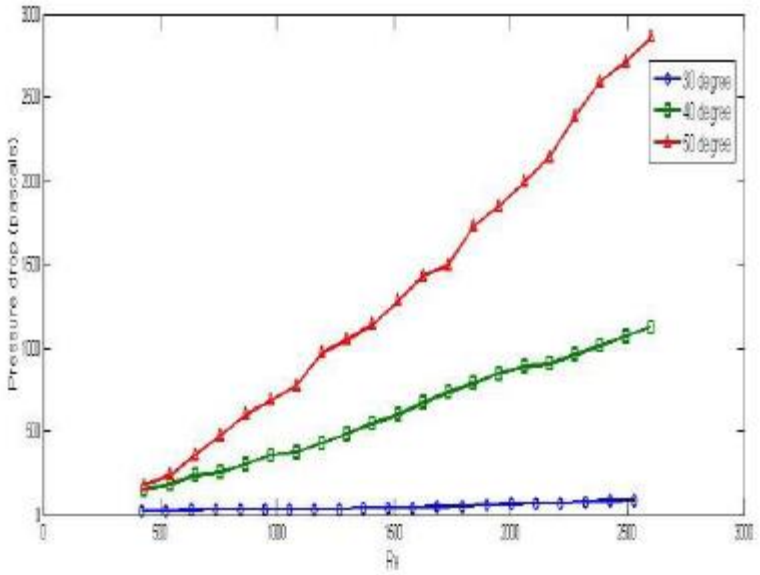

Figure 20 (Reynolds number vs pressure drop) [10].

This article [11]. is about behavioural analysis of velocity boundary layer in a flat plate heat exchanger in laminar flow condition through CFD simulation using fluent software. The aim

was to determine the velocity vectors between the flat plates of heat exchanger. Consequently, some important design features regarding wake point occurrence and pressure loss were investigated. In addition, eddy current and reverse flows in the wake area and the angles of the velocity vectors are described.

For simulation 37240 elements were created with software Gambit. Numerical solution was solved by using finite volume method with Fluent 6.3. Steady flow was entered the channel but at the exit eddy current was observed which is shown in figure 21.

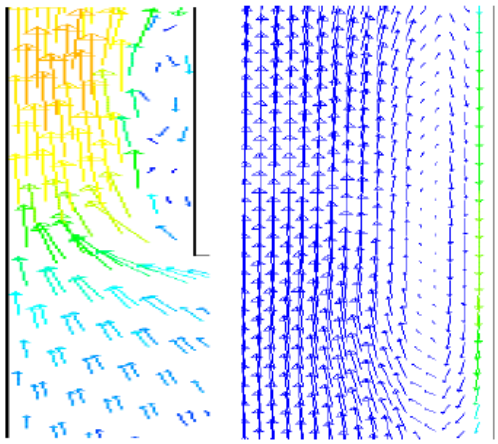

Figure 21 (Observed eddies at outlet) [11].

As conclusion, the pressure of fluid decreases through the flow due to energy losses. Since existence of wake phenomenon and forces exerted on wake area, the probability of corrosion increases and it is better to install measuring devices such as pressure, temperature away from wake area.

3.3.Result

Mentioned articles above are various works about plate heat exchanger for instance, effect of different corrugation angle on pressure drop or pressure drop calculation by using FLUENT software etc. These information is led us for next steps of this study and for following calculations.

4. IDENTIFICATION of CORRUGATION GEOMETRY

4.1. ANALYTICAL SOLUTION

The main aim of this thesis is numerical simulation of existed plate heat exchanger and comparing the numerical results to experimental results which was obtained before. However, we don't have information of dimensions of plate of that heat exchanger because of manufacturer. In order to carry on this study, we must figure out dimensions of plate heat exchanger and then we can design similar model of existed corrugated plate. In other words, that is a kind of reverse engineering study of existed corrugated plates. Therefore, this part of study has major importance.

Size identification of corrugated plate is performed by using formulas from previous part. Here, firstly we estimate required sizes for gap between channels, length, width and port diameter and then we try to get same pressure drop value and heat transfer coefficient which is given in the catalogue. Secondly, pressure drop and heat transfer coefficient are checked according to experimental data results. If result of pressure drop and heat transfer coefficient are same, then estimated sizes are correct.

Catalogue includes thermal properties and its cover dimensions of heat exchanger and these information is not enough to determine exact sizes of plate, however in this part target is estimation of best dimension according to given data. In addition, distance between ports are given in the catalogue and these given dimensions lead us to identify size of corrugated plate. Dimensions of plate cover is given in the figure 22.

	Cold side	Hot Side
Mass Flow Rate	8608.3 kg/h	8602.2 kg/h
Temperature in-out	40-60 °C	75-55 °C
Density	0.988 t/m^3	0.980 t/m^3
Plate Arrangement	1/1*60	1/1*59
Pressure Drop	0.382 Bar	0.384 Bar

Surface	2.7 m^2
Excess Surface	17.72%
Fouling	0.3064 cm^2K/W
Number of plates	120
Conductivity of plates	16 W/(K.m)

Table 2 (Data from manufacturer catalogue)

Figure 22 (Dimensions of heat exchanger cover)

4.1.1 Dimension Determination

Several correlation and formulas are used for calculation and determination of corrugated plate geometry which are shown below. First assumption is that port diameter is estimated as 0.021 mm.

4.1.1.1 Effective Number of Plates (N_e)

Effective number of plates by using equation 1,

N_e=120-2=118

4.1.1.2 Plate Pitch (P)

Plate pitch by using equation 2,

$$p = \frac{L_c}{N_t} = \frac{0.324}{120} = 0.0027\ m$$

4.1.1.3 Mean Channel Gap

Mean channel gap from equation 3,

b=p-t=0.0027-0.0006=0.0021m

4.1.1.4 Hydraulic Diameter (D_h)

Hydraulic diameter from equation 5,

$$D_h = \frac{2b}{\emptyset} = \frac{2 * 0.0021}{1.1772} = 0.003568\ m$$

4.1.1.5 Mass Flow Rate at Each Chanel

Mass flow rate at cold and hot channels are calculated as,

$$\dot{m_{c1}} = \frac{\dot{m}_c}{N_{ch}} = \frac{2.391}{60} = 0.04\ kg/s$$

$$\dot{m_{h1}} = \frac{\dot{m}_h}{N_{ch}} = \frac{2.39}{59} = 0.041\ kg/s$$

Where m_{c1} and m_{h1} are mass flow rate at each cold and hot channels.

4.1.1.5 Mass Velocities

Calculated by using equation 7.

$$G_c = \frac{\dot{m}_{c1}}{bW_p} = \frac{0.04}{0.0021 * 0.0715} = 265.5\ (\frac{kg}{m^2 s})$$

$$G_h = \frac{\dot{m}_{h1}}{bW_p} = \frac{0.041}{0.0021 * 0.0715} = 269.7\ (\frac{kg}{m^2 s})$$

Where, W_p is width of the plate.

4.1.1.6 Reynolds Number

Reynolds number is calculated by using equation 12.

$$Re_c = \frac{G_c D_h}{\mu_c} = \frac{265.5 * 0.003568}{0.000547} = 2038.2$$

$$Re_h = \frac{G_h D_h}{\mu_h} = \frac{265.5 * 0.003568}{0.000547} = 2616.2$$

Where Re_c and Re_h are Reynolds numbers at hot and cold sides. Since Reynold number is greater than 1000 for both cold and hot side, flow is turbulent.

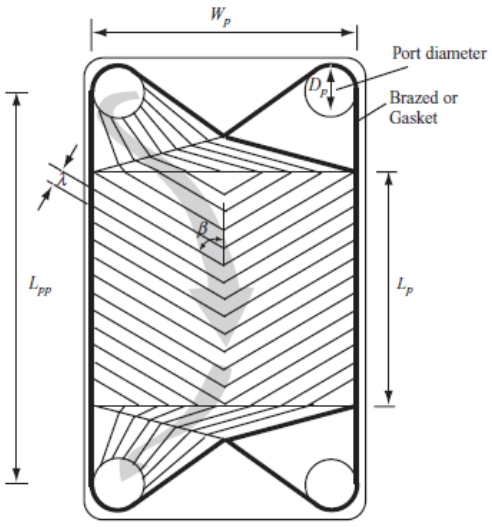

Figure 23 (Geometry of corrugated plate) [6].

4.1.1.7 Corrugation Pitch

By using equations 3 and 4, corrugation pitch is calculated as,

λ =7.44 mm

Determined Sizes

Determined parameters are;

D_p= 21 mm

L_{pp}= 250 mm (given from catalogue)

W_p = 71 mm

λ =7.44 mm

4.2. Pressure Drop and Nusselt Number Calculations for Catalogue

There are numerous correlation to calculate pressure drop and Nusselt Number which depend on corrugation geometry, sizes of plate and flow regime.

The overall pressure drop of plate heat exchanger consists of the pressure drop at inlet and outlet ports and pressure drop in channels. The pressure drop due to potential energy lost is neglected in our calculation.

4.2.1 Pressure Drop at Ports

Calculation of pressure drop at port for cold and sides by using equations 7 and 37.

For cold side,

$$G_{pc} = \frac{4 * 2.391}{\pi * 0.021^2} = 6590.5 \, (\frac{kg}{m^2 \, s})$$

$$\Delta P_{pc} = \frac{1.5 * 6590.5^2}{2 * 988.1} = 32.968 \, kPa$$

For hot side,

$$G_{ph} = \frac{4 * 2.39}{\pi * 0.021^2} = 6584.6 \, (\frac{kg}{m^2 \, s})$$

$$\Delta P_{ph} = \frac{1.5 * 6584.6^2}{2 * 980.4} = 33.168 \, kPa$$

In order to calculate pressure drop at channel, equation 38 is used but before that friction factor should be calculated. There are several correlation for determination of friction factor and calculation is performed by using these correlations, then we choose the best fitted formulas for pressure drop value in catalogue.

4.2.2 Pressure Drop at Channel

In this step, we should estimate chevron corrugation angle as well. Estimation is carried out most common chevron angles such as 30^o, 45^o and 60^o.

To determine friction factor (*f*), we use two different correlations which are shown below.

a) According to Mulley Correlation

Friction factor and Nusselt number are calculated by equations 39 and 40.

Cold Side	ϐ (degree)	ϐ (radian)	Nu	f	ΔPch	ΔPp (Pa)	ΔP (Pa)	ΔP (kPa)	ΔP (bar)
	30	0.52	28.16	0.173	1756.4	36222	37979	37.98	0.380
	45	0.79	34.62	0.241	2439.4	36222	38662	38.66	0.387
	60	1.05	46.11	0.329	3339.6	36222	39562	39.56	0.396
hot Side	30	0.52	30.82	0.167	1760.3	36442	38202	38.20	0.382
	45	0.79	38.41	0.232	2444.7	36442	38886	38.89	0.389
	60	1.05	51.48	0.313	3305.3	36442	39747	39.75	0.397

Table 3 (Result of pressure drop values)

Calculated values are 0.396 Bar for cold side and 0.397 Bar for hot side

b) According to Martin Correlation

Applying equations 41 and 42 for estimated parameters, we obtain following results. Calculated values according to Martin Equation are given in the table 4 below.

Martin Equatıon						Total Pressure			
Cold Side	f0	f1	f	Nu	ΔPch	ΔPp (Pa)	ΔP (Pa)	ΔP (kPa)	ΔP (bar)
	0.01	1.04	0.10	37.9	1034.7	36222.3	37257.0	37.3	0.373
	0.01	1.04	0.21	52.2	2109.8	36222.3	38332.1	38.3	0.383
	0.01	1.04	0.47	67.1	4757.8	36222.3	40980.1	41.0	0.410
Hot Sıde									
	0.01	1.00	0.11	42.78	1133.4	36441.7	37575.1	37.6	0.376
	0.01	1.00	0.22	58.65	2281.6	36441.7	38723.3	38.7	0.387
	0.01	1.00	0.48	75.08	5100.2	36441.7	41541.9	41.5	0.415

Table 4 (Result of pressure drop values)

For Pressure drop, 0.41 bar for cold side and 0.415 bar have been calculated for catalogue input data.

4.3 Pressure Drop and Nusselt Number Calculations for Measurement

Required dimensions were calculated so far, however that is not enough whether determined dimensions are correct or not. Therefore, pressure drop and heat transfer calculations must be checked against for different flow rates and temperature difference of another stream. Then we can use measurement data which was carried out before in department laboratory in same heat exchanger. Measurement parameters and results are given in the appendix C. Calculation for measurement 28 is shown here and other calculations are given in appendix B.

4.3.1 Pressure Drop at Ports

Calculation procedure is same as previous pressure drop for ports, hence taken results are also same.

4.3.2. Pressure Drop at Channels

a) According to Martin Equation

Calculations are performed according to equations 41 and 42.

Martin Equation							***Total Pressure***		
Cold Side	***f0***	***f1***	***f***	***Nu***	***ΔPch***	***ΔPp (Pa)***	***ΔP (Pa)***	***ΔP (kPa)***	***ΔP (bar)***
	0.016	1.11	0.58	48.70	2858.73	17586.26	20445.0	20.4	0.204
	0.016	1.11	0.69	54.84	3399.33	17586.26	20985.6	21.0	0.210
	0.016	1.11	0.85	56.05	4162.37	17586.26	21748.6	21.7	0.217
Hot Side									
	0.016	1.28	0.58	51.90	3258.8	19373.6	22632.4	22.6	0.226
	0.016	1.28	0.69	58.47	3881.4	19373.6	23255.0	23.3	0.233
	0.016	1.28	0.85	59.85	4770.4	19373.6	24144.0	24.1	0.241

Table 5 (Calculation results of Martin Equation)

For given estimated geometry, we calculated these values as 0.217 bar at cold side and 0.241 bar at hot side shown in table 5.

Calculated overall heat transfer coefficients are given in table….below.

Angel	*h_c (W/m2K)*	*h_h ((W/m2K)*	*U (W/m2K)*
30	8422.7	9018.7	3743.8
45	9483.0	10160.3	4143.0
60	9693.4	10400.1	4222.7

Table 6 (Heat transfer coefficients)

b) According to table

The range of Mulley Correlation is not suitable for measurement calculations because of Reynolds number range and instead of that we use another correlations which are equations 43 and 44.

Heat transfer coefficient:

Angle	60
f_c	0.84
f_h	0.83
Nu_c	59.1
Nu_h	62.42
h_c (W/[m^2K])	10222.32
h_h (W/[m^2K])	10846.6
U (W/[m^2K])	4395.2

Table 7 (Calculation results for heat transfer coefficient and friction factor)

Pressure drop:

	ΔPch	ΔPp (Pa)	ΔP (Pa)	ΔP (kPa)	ΔP (bar)
cold side	4097.9	16006.5	20104.4	20.1	0.201
warm side	4020.3	17633.3	21653.6	21.7	0.217

Table 8 (Calculated values for friction factor)

By this method, for pressure drop we obtained 0.201 bar at cold side and 0.217 bar at hot side which is given in table 8 above.

4.4 Dimensions of Plate Heat Exchanger

Three dimensional plate drawing has been carried out on software Solidworks 2013. According to identified dimensions, construction of three dimensional model of plates have been drawn. Drawing of corrugated plate is given below in figure 24 and 25. Total length of plate was estimated as 275 mm

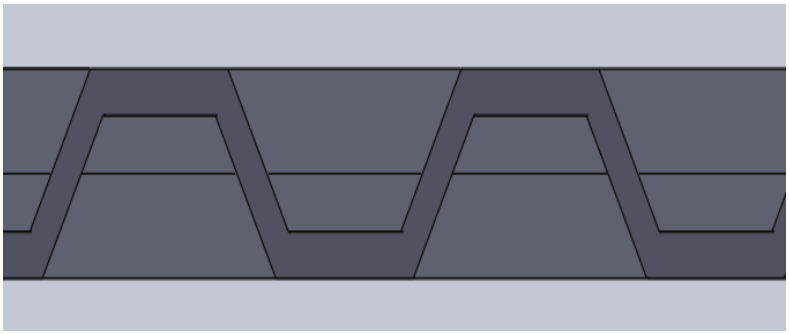

Figure 24 (Created first model)

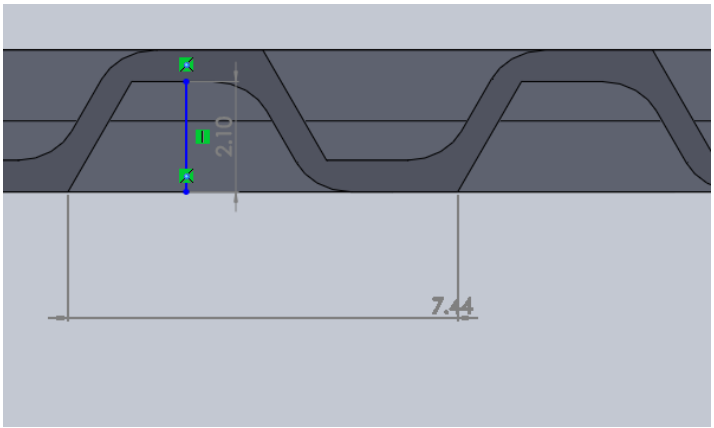

Figure 25 (Side view of plate with radius)

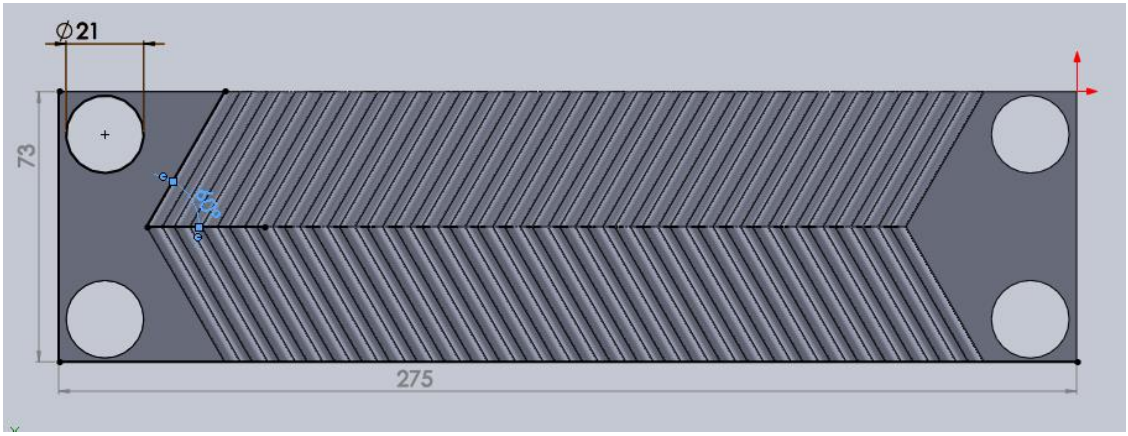

Figure 26 (Top view of plate)

In order to draw inlet and outlet ports, width of the plate is increased from 71 mm to 73 mm. In addition, for decreasing pressure drop in channel, 0.5 mm radius is given to sharp corners however that operation hasn't been possible for all sharp corners since small impurities remained after the operation and that is the problem during the mesh process.

5. DESCRIPTION of EXPERIMENT

Data of measurement is focal point of this study and it consists of 40 district measurements. However, we asses some of these measurements and compare results of analytical and numerical solutions. Data and results of measurement are given in the table 9, 10 and 11 below [13].

Measurement conditions:		
Date	23/01/2015	
Temperature	17.5	°C
Water density	995	kg/m^3
Heat capacity	4183	J/kg K
Area	2.7	m^2

Table 9 (Conditions of experiment)

Measured data			
		Hot side	Cold side
Flowrate beginning	Q (m^3/h)	6.3	6.03
Flowrate end	Q (m^3/h)	6.4	6.07
Pressure drop	∆p (bar)	0.246	0.225

Table 10 (Results of measurement)

In the data, volume flow rate is given, and firstly we should convert it to mass flow rate by multiplying density at given condition.

$$\dot{m_h} = \frac{6.3 * 995}{3600} = 1.755\ kg/s$$

$$\dot{m_c} = \frac{6.03 * 995}{3600} = 1.672\ kg/s$$

Where $\dot{m}_c$ and $\dot{m}_h$ are mass flow rates at hot and cold inlets.

There are 59 passages at hot stream and 60 passages for cold streams. Mass flow rates at each hot and cold passages,

$$\dot{m}_{h1} = \frac{1.755}{59} = 0.02975\ kg/s$$

$$\dot{m}_{c1} = \frac{1.672}{60} = 0.02787\ kg/$$

Pressure drop value is 246 *kPa* for hot side and 225 *kPa* for cold side. By using equation 36, we can calculate pressure drop at channels. From table 5, pressure drop at cold side is 17586.3 Pa and at cold side pressure drop is 19373.6 Pa.

$$\Delta Pc_c = 22500 - 17586.3 = 4913.7 \text{ Pa}$$

$$\Delta Pc_h = 24600 - 19373.6 = 5226.4 \text{ Pa}$$

Where, ΔPc_c and ΔPc_h are pressure drops at channels for cold and hot sides.

	Temperature °C										
	Hot side		Cold side								
No of measurement	IN	OUT	IN	OUT	ΔT_T (°C)	ΔT_S (°C)	Q_T (W)	Q_S (W)	ΔQ (W)	ΔT_{ln} (°C)	k (W/m²K)
1	46.4	39	27.3	44.1	7.4	16.8	54755	117898	63143	5.78	5533
2	46.5	31.5	22.3	38.7	15	16.4	110989	115091	4102	8.48	4937
3	46	32.3	24.2	39.2	13.7	15	101370	105266	3896	7.43	5149
4	43.1	31.8	24.3	37.6	11.3	13.3	83612	93336	9724	6.45	5082
5	41.3	31.3	25	36.3	10	11.3	73993	79300	5308	5.62	5047
6	40.4	31.1	25.5	35.8	9.3	10.3	68813	72283	3470	5.08	5140
7	39.8	31.2	25.8	35.2	8.6	9.4	63634	65967	2333	4.99	4810
8	38.6	31	26.1	34.7	7.6	8.6	56234	60353	4118	4.38	4928
9	38.2	30.8	26.4	34.4	7.4	8	54755	56142	1387	4.09	5018
10	37.6	31.1	26.6	34.3	6.5	7.7	48095	54037	5941	3.87	4888
11	37.6	31.1	26.9	34	6.5	7.1	48095	49826	1731	3.89	4659
12	37.2	31	27.1	33.9	6.2	6.8	45875	47721	1845	3.59	4826
13	36.7	30.9	27.6	33.5	5.8	5.9	42916	41405	1511	3.25	4805
14	36.2	31	27.7	33.5	5.2	5.8	38476	40703	2227	2.99	4904
15	35.6	30.9	27.9	33	4.7	5.1	34777	35790	1014	2.80	4675
16	35.6	30.8	28	33	4.8	5	35516	35089	428	2.70	4845
17	35.4	31.1	28.3	33	4.3	4.7	31817	32983	1167	2.59	4625
18	35.4	31.1	28.5	33.2	4.3	4.7	31817	32983	1167	2.39	5012
19	35.2	31.1	28.6	32.9	4.1	4.3	30337	30176	161	2.40	4672
20	35.3	31.1	28.6	33.1	4.2	4.5	31077	31580	503	2.35	4944
21	34.9	31.1	28.7	32.9	3.8	4.2	28117	29474	1357	2.19	4861
22	34.9	31.1	28.9	32.8	3.8	3.9	28117	27369	748	2.15	4780
23	34.8	31.3	29.1	33	3.5	3.9	25897	27369	1472	1.99	4949
24	34.6	31.2	29.3	33	3.4	3.7	25157	25966	808	1.75	5423
25	34.6	31.3	29.3	33	3.3	3.7	24418	25966	1548	1.79	5205
26	34.3	31.4	29.5	32.5	2.9	3	21458	21053	405	1.85	4256

27	34.4	31.4	29.7	33	3	3.3	22198	23159	961	1.55	5436
28	34.3	31.6	29.7	32.5	2.7	2.8	19978	19650	328	1.85	3968
29	34.1	31.3	29.8	32.9	2.8	3.1	20718	21755	1037	1.34	5850
30	34.2	31.6	29.8	32.7	2.6	2.9	19238	20351	1113	1.65	4456
31	34	31.9	30	32.6	2.1	2.6	15538	18246	2708	1.64	3821
32	34.2	31.6	30	32.9	2.6	2.9	19238	20351	1113	1.44	5074
33	34.2	31.5	30.1	32.7	2.7	2.6	19978	18246	1732	1.45	4884
34	34.2	31.8	30.1	32.8	2.4	2.7	17758	18948	1190	1.55	4399
35	34.4	31.6	30.2	33.1	2.8	2.9	20718	20351	366	1.35	5636
36	34.2	31.7	30.1	32.9	2.5	2.8	18498	19650	1152	1.44	4889
37	34.2	31.7	30.4	33.1	2.5	2.7	18498	18948	450	1.20	5792
38	34	31.9	30.6	32.9	2.1	2.3	15538	16141	602	1.20	4900
39	34.1	31.8	30.6	32.8	2.3	2.2	17018	15439	1579	1.25	4811
40	34.2	32	30.6	33	2.2	2.4	16278	16843	564	1.30	4727

Table 11 (Measurements)

In the table, ΔT_T and ΔT_S are temperature differences for hot and cold streams, Q_T and Q_S are heat fluxes of hot and cold streams and ΔT_{ln} is logarithmic mean temperature.

6. RESULTS from ANALYTICAL SOLUTION

6.1. Results from Catalogue

6.1.1. According to Mulley Correlation

Overall pressure drop values according to catalogue (see table 2) are 0.382 bar for cold side and 0.384 bar hot side and we calculated similar values for 60^o. Calculated values are 0.396 Bar for cold side and 0.397 Bar for hot side. Error for calculated values are approximately 4 % thus, results are acceptable.

However, for overall heat transfer coefficient (see in appendix A), calculated value is 3.407 kW/[m^2K] and catalogue value is 4.913 kW/[m^2K] and error is around 30 % and that value is not acceptable.

6.1.2. According to Martin Correlation

For Pressure drop, we obtained 0.4 bar for cold side and 0.41bar for cold side. Results are greater than Mulley equation but error is approximately less than 5%. For heat transfer coefficient, we obtained 4.4787 kW/m^2K (see appendix A) and obtained heat transfer coefficient value is so close to value of catalogue. Error is approximately 9% for heat transfer coefficient.

6.2 Results from Measurement

6.2.2 According to Martin Correlation

According to measurement data, pressure drop for cold side is 0.225 bar and for hot side 0.246 bar. For given estimated geometry, we calculated these values as 0.217 bar at cold side and 0.241 bar at hot side. Heat transfer coefficient from measurement was given as 3968 W/m^2K and we obtained this value as 4227.4 W/m^2K (see appendix B). Errors are negligible (less than 10 %).

6.2.3 According to table

From table, for pressure drop we obtained 0.217 bar at cold side and 0.234 bar at hot side. Heat transfer coefficient is obtained as 4412.2 W/[m^2K]. Again errors are less than 5 % for pressure

drop and less than 10 % for heat transfer coefficient .Results show that our estimated size values are nearly correct.

6.3 Determined Result Comparison

Calculated results and their comparisons are given in the tables 12, 13, 14 and 15 below. For comparison, several measurements have been selected which have less energy losses than other measurements.

Number of Measurement	*ΔP Experiment (Bar)*		*Martin Equation (Bar)*		*From Table (Bar)*	
	Cold Side	*Hot Side*	*Cold Side*	*Hot Side*	*Cold Side*	*Hot Side*
Measurement 16	0.225	0.246	0.218	0.241	0.217	0.235
Measurement 19	0.225	0.246	0.217	0.241	0.217	0.234
Measurement 20	0.225	0.246	0.217	0.241	0.217	0.234
Measurement 26	0.225	0.246	0.217	0.241	0.217	0.234
Measurement 28	0.225	0.246	0.217	0.241	0.217	0.234
Measurement 35	0.225	0.246	0.217	0.241	0.217	0.234
Measurement 37	0.225	0.246	0.217	0.241	0.217	0.234
Measurement 38	0.225	0.246	0.217	0.241	0.217	0.234
Measurement 40	0.225	0.246	0.217	0.241	0.217	0.234

Table 12 (Calculated pressure drop values)

	Martin Equation. Error %		*Table Error %*	
	Cold Side	*Hot Side*	*Cold Side*	*Hot Side*
Measurement 16	3.3	1.8	3.3	4.6
Measurement 19	3.3	1.8	3.4	4.7
Measurement 20	3.3	1.9	3.4	4.7
Measurement 26	3.3	1.9	3.4	4.7
Measurement 28	3.3	1.9	3.4	4.7
Measurement 35	3.3	1.9	3.4	4.7
Measurement 37	3.4	1.9	3.4	4.7

Measurement 38	3.4	1.9	3.4	4.7
Measurement 40	3.4	1.9	3.4	4.7

Table 13 (Comparison for pressure drop)

Heat Transfer Coefficients W/[Km²]			
Number of Measurement			
	Experiment	***Martin Equation***	***From Table***
Measurement 16	4845	4173.3	4368.8
Measurement 19	4672	4218.1	4408.2
Measurement 20	4944	4223.7	4413.5
Measurement 26	4256	4218.2	4408.3
Measurement 28	3968	4222.7	4412.3
Measurement 35	5636	4233.2	4421.6
Measurement 37	5792	4234.3	4422.4
Measurement 38	4900	4236.6	4422.4
Measurement 40	4727	4236.6	4424.4

Table 14 (Calculated heat transfer coefficient values)

Error %	
Martin Equation	***From Table***
13.9	9.8
9.7	5.6
14.6	10.7
0.9	-3.6
-6.4	-11.2
24.9	21.5
26.9	23.6
13.5	9.7
10.4	6.4

Table 15 (Heat transfer coefficient comparison)

6.3.1 Result

As mentioned before, lack of dimension information, we try to estimate the best fitted approximation for geometry determination of corrugated plate. As seen above from tables, estimations look desirable.

7. CFD SIMULATION

7.1 MODEL

7.1.1 Plate Model and Fluid Domain Creation

The first step of numerical simulation is creating model of corrugated plate and then creation of fluid domain between two plates. The geometry considered consists of inlet and outlet ports and cross-corrugated channels. Construction of the cross-corrugated plates and creation of fluid domain were carried out by using software Solidworks 2013 according to obtained dimensions, which is described in previous section. Since lack of information about geometry about plate, gasket is neglected during the drawing process. Created fluid domain is given in figure 27 below.

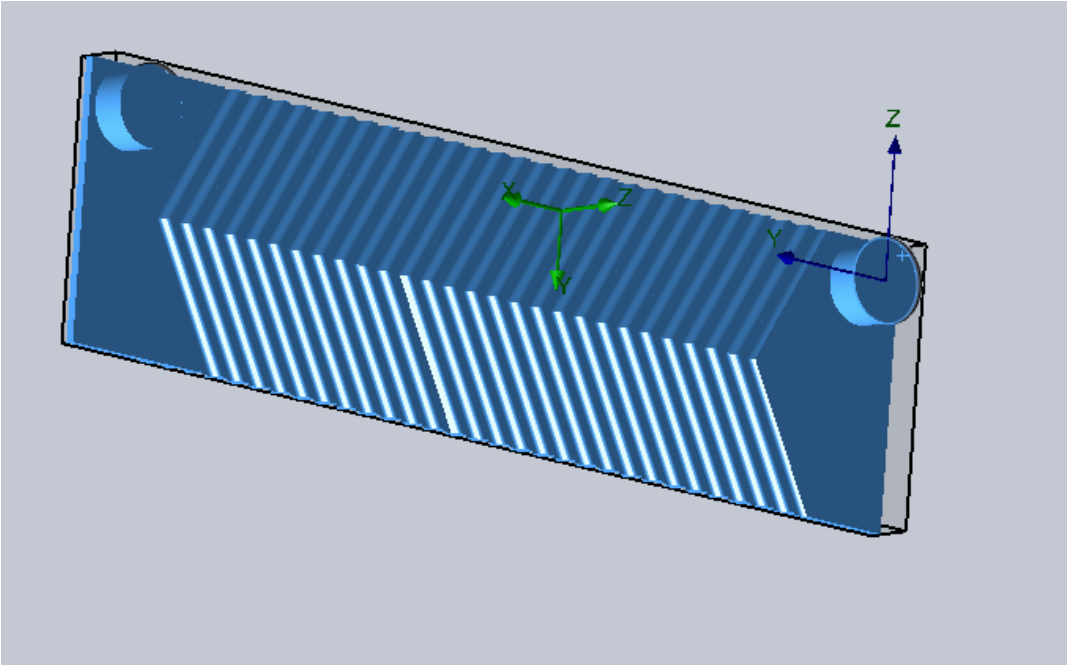

Figure 27 (Created fluid domain)

7.1.2 Mesh

The partial differential equations that govern fluid flow and heat transfer are not usually reasonable to analytical solutions, except for very simple cases. Therefore, in order to analyse fluid flows, flow domains are split into smaller subdomains. The governing equations are then discretised and solved inside each of these subdomains. The subdomains are often called elements or cells, and the collection of all elements or cells is called a mesh or grid. Therefore

quality of mesh and number of elements in mesh model have major importance to get correct results from simulated model.

In this study, 2 different mesh models have been created with different mesh sizes and different number of elements. Aim of creating two different mesh is to find out the best fitted model. Actually, we need more than 2 mesh models for that process but because of time constrain and some problems about computer, we couldn't have created more than two mesh model. Mesh generation has been carried on fluid domain. For all mesh models, tetrahedral elements have been created for computational grid to describe complexity of the corrugated passage. Mesh generation has been implemented in ANSYS software.

For first mesh model of trapezoidal corrugated plate in which 816 764 number of elements have been created by patch conforming method which is given in figure 28. Orthogonal mesh quality is approximately 0.13, value of skewness is $8.14*10^{-6}$ and curvature normal angle is $32{,}5^{o}$ and statistical parameters are given in table 11 below.

Figure 28 (First mesh model)

Statistics	
Nodes	185950
Elements	816764
Mesh Metric	Orthogonal Quality
Min	0.127304940375556
Max	0.995477424966341
Average	0.842184663130338
Standard Deviation	9.59632189227109E-02

Table 16 (Statistical values of first mesh model)

The second mesh model has lower number of elements than first mesh model. Orthogonal quality is 0.15 and curvature normal angle is 40°. 816 764 number of elements have been created. Statistical parameters are given in table 17 below. Face sizing has been chosen for mesh size. Obtained mesh model is given in the figure 29 below.

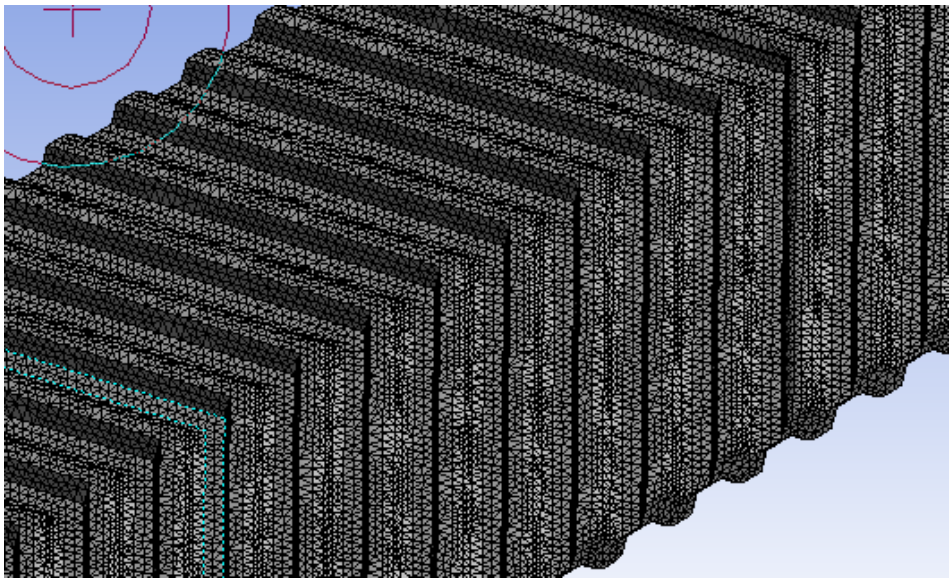

Figure 29 (Second mesh model)

Statistics	
Nodes	136638
Elements	574719
Mesh Metric	Skewness
Min	4.10973811815207E-06
Max	0.939889879052956
Average	0.266728839012829
Standard Deviation	0.147838809618802

Table 17 (Statistical values of second mesh model)

7.1.3 Simulation

Aim is numerical solution of model of fluid domain between corrugated plates. Three dimensional simulation is done for lab measurement number 37 at hot inlet and outlet streams and simulation has been performed for both mesh models and reason is heat loss is less than other measurements. Model is simulated for one passage of plate heat exchanger. Numerical simulation is carried on software Fluent 15. The flow is assumed to be steady, turbulent and

three-dimensional. Reynolds number is greater than 1000, thus turbulent k-ε model is selected. Standard wall function is used to calculate the variables at the near wall cells. For the boundary conditions the flow at the inlet port selected as flow rate and pressure outlet for outlet port. Parameters of measurement number 37 is given in the table 16 below.

Hot side temperatures		Unit
Th_i	34.2	^oC
Th_o	31.7	^oC
Th_m	32.95	^oC
ρ_h	995	kg/m^3
c_c	4.18	kJ/(kg*K)
ϑ_h	0.000749	Pa.s
Mass flow rate	0.02975	kg/s
Reynold hot side	1110.9	
Pr number (hot)	5.05	

Table 18 (Parameters of measurement 37)

7.2 RESULTS

7.2.1 Results for First Mesh model

Simulation results of first mesh model is explained in this part. Obtained results, pressure and temperature profiles are given in figure 30 and 31 below.

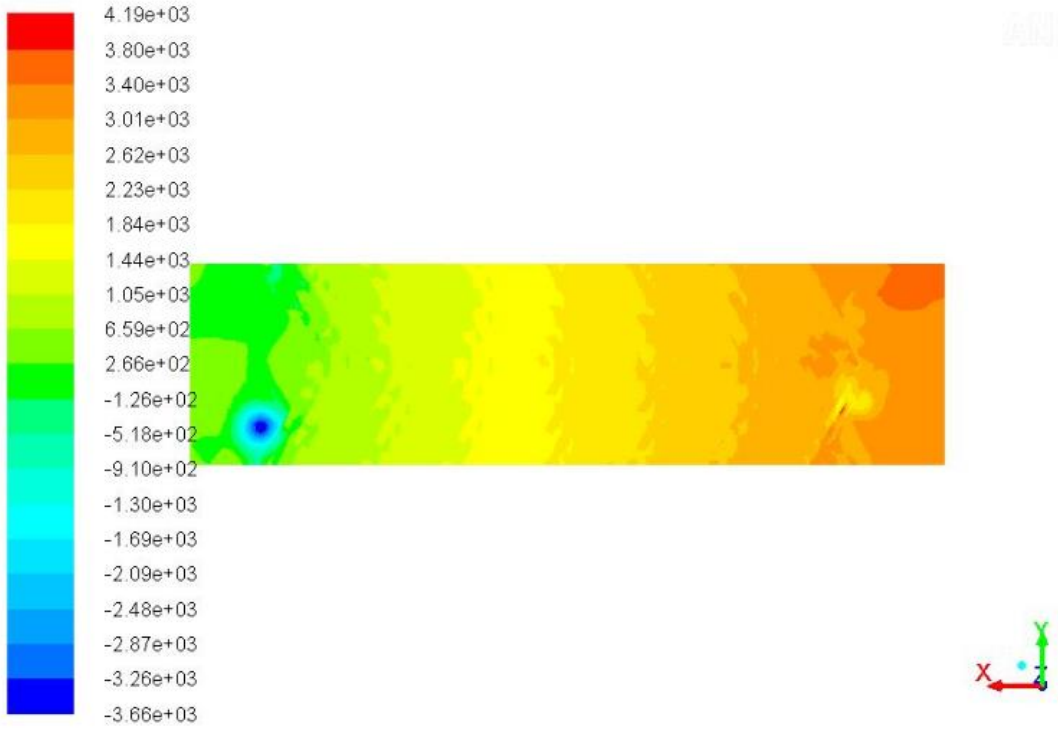

Figure 30 (Pressure Profile for first mesh model)

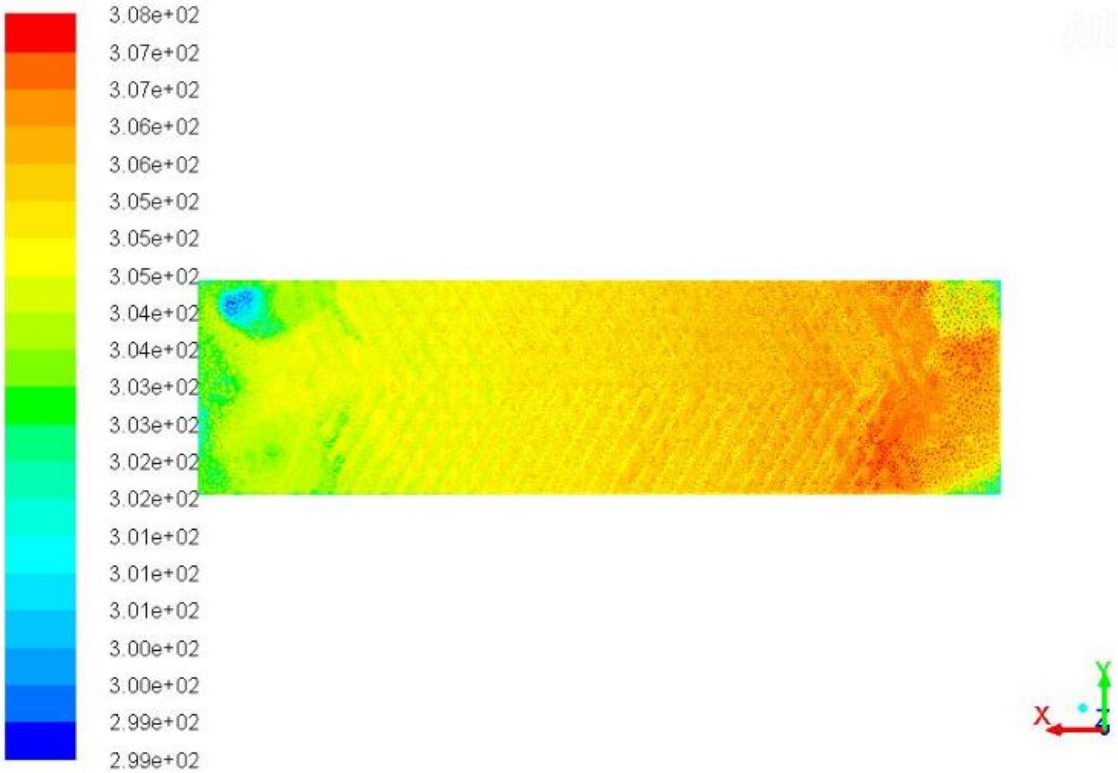

Figure 31 (Temperature profile of first mesh model)

Pressure		
Inlet	341208	Pascal
Outlet	-2.2	Pascal
ΔP	3415	Pascal
Temperature		
Temperature in	307.4	Kelvin
Temperature out	301.1	Kelvin

Table 19(Results of pressure and temperature for first mesh model)

As seen from tables above, pressure drop is calculated as 341208 Pa and temperature at outlet as determined as 27.9^{o} C.

7.2.2 Results for Second Mesh Model

Simulation of second mesh model is described in this part. Obtained results, pressure and temperature profiles are given below in figure 32 and 33 below.

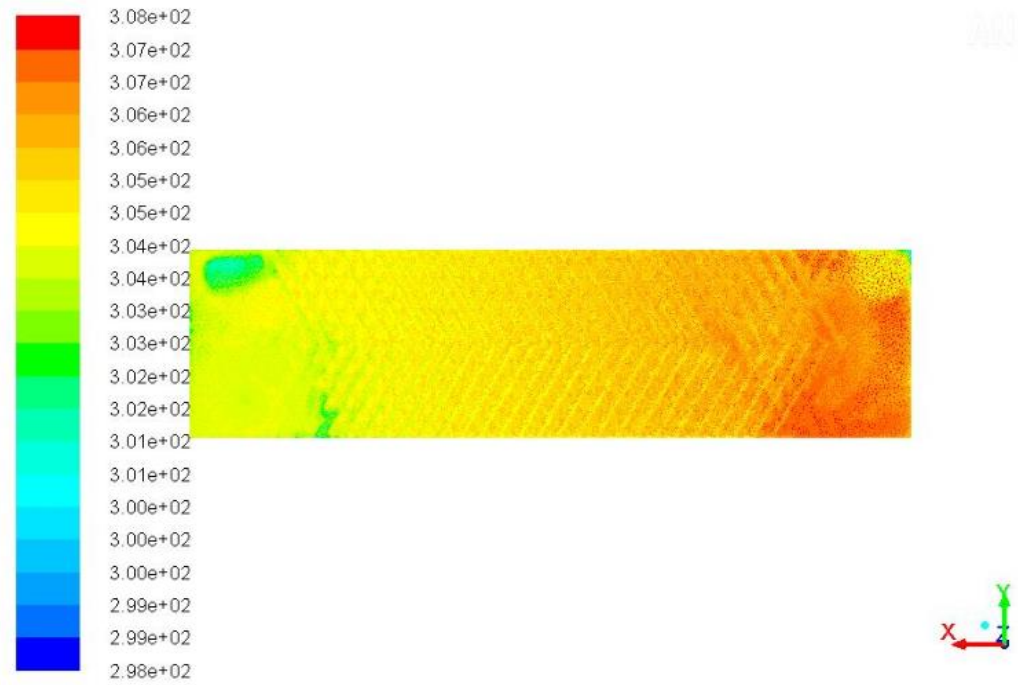

Figure 32(Temperature profile of second mesh model)

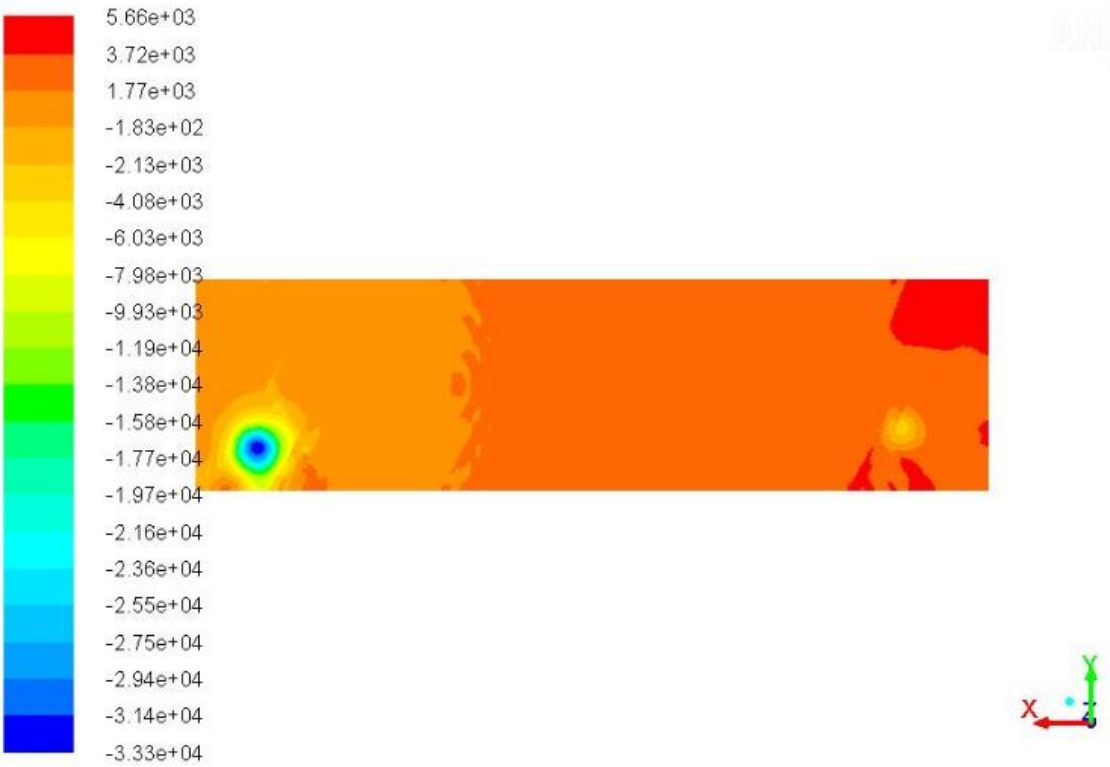

Figure 33 (Pressure Profile of second mesh model)

Pressure		
Inlet	3989.1	Pascal
Outlet	-10.7	Pascal
ΔP	400	Pascal
Temperature		
Temperature in	307.4	Kelvin
Temperature out	301.5	Kelvin

Table 20 (Results of pressure and temperature for second model)

As seen from table 20 above, pressure drop is calculated as 4000 Pas and outlet temperature has been determined as 28.3 ^{o}C.

8. COMPARISON

Two different mesh models were created and their number of elements are different than each other. Therefore different pressure drop and outlet temperature values were taken.

In first model, pressure drop was taken as 3412.8 Pa and this is much more different than result of analytical solution and experimental result. Error is 35% comparing to experimental result. We can see that this model is not so desirable for pressure drop calculation. Outlet temperature value is obtained as 27.9 ^{o}C and that values are much different than experimental result.

Pressure drop value was determined as 4000 Pa for second mesh model and pressure drop value for analytic calculation is 4072 Pa which is given in the table 5. From measurement, pressure drop value was calculated as 5226.4 Pa. Results from simulation and analytical solution are so close to each other and result from experiment is approximately 23 % different than numerical result.. According to article of Ying-Chi Tsai, Fung-Bao Lu [2], the difference between experimental and numerical results had been calculated as 20 % for similar study with known geometry. For our case, 23 % difference for pressure drop can be acceptable.

Value of outlet temperature is determined as 28.3 ^{o}C and outlet temperature result of measured value is 31.7 ^{o}C and difference is 3.4 ^{o}C. Unfortunately these values are not close to each other. This result shows that, created geometry model is not acceptable. Model satisfies for pressure drop but not for temperature difference. Second model shows that mesh structure and its quality has a major importance, even for same input values, we got totally different results from second model

	Outlet temperature ^{o}C	ΔP (Pascal)	Error % for ΔP	Error % for T
Experiment	31.7	5226.4		
1. Mesh Model	28.3	4000	23	11
2.Mesh Model	27.9	3412.8	35	12

Table 21(Comparison of numerical and measurement results)

9. CONCLUSION

Aim of this study was designing a model of plate heat exchanger in software ANSYS and performing a simulation for given parameters. However, geometry and dimensions of corrugated plate were not known. Therefore, geometry and dimensions of corrugated plate must have determined, and first of all analytic determination was carried out according to manufacturer catalogue and secondly experimental measurement data which had performed before.

Dimensions were estimated and checked for measurement data and result was satisfied measurement results. After that three dimensional geometry of corrugated plate was drawn in Solidworks 2013 and fluid domain was created between two plates.

Numerical simulation was carried out by using constructed model of corrugated plates. During the numerical simulation only one passage was used and two models were created with different mesh parameters in which one of them has different number of elements than other mesh model. Results of numerical simulation was compared with analytical solution and experimental results. Model with less dense mesh was satisfied for pressure drop value. Result for pressure drop was nearly acceptable but model was failed for thermal calculation. Different outlet temperatures were obtained from simulation. The first model with dense mesh were not satisfied for both pressure drop value and thermal characteristic. It is clear that, quality of created geometry is poor. In order to get better results, geometry of plate must be improved. In addition, more than two mesh model should be created to obtain a desirable comparison.

REFERENCES

[1] Nasir Hayat, Muhammad Mahmud Aslam Bhutta, CFD Application in Various Heat Exchanger Design, Applied Thermal Engineering 32, (2011) 1-11.

[2] Ying-Chi Tsai, Fung-Bao Lu, Po-Tsun Shen, Investigation of Pressure Drop and Flow Distribution in a Chevron Type Plate Heat Exchanger, International Communications in Heat and Mass Transfer 36, (2009) 574-578.

[3] F. Akturk, G. Gulben, S.Kakac, Experimental Investigation of the Characteristics of a Chevron Type Gasketed Plate heat Exchanger, 6th.International Advanced Technologies Symposium Turkey, (2011) 172-178.

[4] Aydin Durmus, Huseyin Benli, Hasan Gul, Investigation of Heat Transfer and Pressure Drop in Plate Heat Exchangers Having Different Surface Profile, International Journal of Heat and Mass Transfer 52, (2007) 1451-1457.

[5] A. Muley, R.M. Manglik, Experimental Study of Turbulent Flow Heat Transfer and Pressure Drop in Plate Heat Exchanger with Chevron Plates, Journal of Heat Transfer, (1999) 110-116

[6] HoSung Lee, Thermal Design, (2010) 285-290.

[7] Ramesh K. Shah and Dusan P. Sekulic, Fundamentals of Heat Exchangers, (2003) 632-637.

[8] Sadik Kakac, Hongtan Liu, Heat Exchangers, (2002), 380-404.

[9] Yunus A. Cengel, Afshin J. Ghajar, Heat and Mass Transfer, Fourth Edition, 2011

[10] B. Sreedhena Raa, Verus S. Experimental Studies on Pressure Drop in a Sinusoidal Plate Heat Exchanger, International Journal of Research in Engineering and Technology, (2014), 122-126

[11] Mojtaba Mirddrikwand, Behrooz Roozbehani, S. Imani Moqadam, Velocity Boundary Layer Analysis of a Flat Plate Heat Exchanger in Laminar Flow, Engineering, Technology & Applied Science Research, (2012), 310-314

[12] http://investors.ansys.com/events-and-presentation

[13] Moravec J, Dostal M, Process Characteristics Measurement of plate Heat Exchanger

LIST of TABLES

LIST of FIGURES